ISSN 2616-5872 Vol.7, Issue 4: 9-25, DOI: 10.25236/AJEE.2025.070402

Atmospheric Formaldehyde Column Concentrations from Multi-Satellites Data Observations over Egypt, 1997-2021

Guanghui Zheng[a], Tianzhen Ju[b,*], Yumeng Qiu[c], Jiachen Li[d], Zhichao Lv[e]

College of Geography and Environmental Sciences, Northwest Normal University, 730070, No.27, Qiujiawan, Anning District, Lanzhou City, Gansu Province, China
[a]631782338@qq.com, [b]jutianzhen@nwnu.edu.cn, [c]1203861047@qq.com, [d]2022213029@nwnu.edu.cn, [e]2760679951@qq.com
**Corresponding author*

Abstract: *Spatial and temporal variations of tropospheric formaldehyde (HCHO) column concentrations over Egypt during 1997-2021 based on multi-satellites observations is presented. The HCHO growth rates are analyzed and the influencing factors of HCHO such as, vegetation presented by the NDVI (normalized difference vegetation index), meteorology and backward trajectories for qualitatively exploring the impacts of natural and anthropogenic emissions on HCHO variations are also addressed. The main results are: the annual average HCHO column concentrations in the Egyptian region is* 3.71×10^{15}~ 9×10^{15}*molec/cm*^{2}*, and the highest values are mainly concentrated in the Nile Delta, immediately followed by in the North Mediterranean coast, Sinai Peninsula, and the eastern coastal areas, while the lowest values are found in the desert areas of the south-west. The annual HCHO concentrations showed an overall increasing trend from 1997 to 2021, with highest (lowest) values in summer (winter). Among the natural factors, the HCHO geographical gradient differences are mainly influenced by the combination of wind, vegetation and marine factors. Industrial emissions, and economic activities enhanced the HCHO growth rate be higher in the Nile Delta cities than in other cities, and the rate is strongly correlated with the increase of atmospheric methane.*

Keywords: *HCHO Column Concentration, Temporal and Spatial Distribution, Growth Rate, Egypt*

1. Introduction

Formaldehyde (HCHO) is one of the major volatile organic compounds (VOCs) and an important source of free radicals such as HO_2 and OH in troposphere, thus HCHO plays a sinificant role in the formation of atmospheric photochemical pollution, secondary aerosols, and acid rain. HCHO is also a common air pollutant with a potential hazard to human health. Primary sources of HCHO are anthropogenic emissions, such as the combustion of fossil fuels and the release of construction materials or certain natural processes. The secondary source is the photochemical oxidation of atmospheric VOCs (e.g. isoprene, monoterpenes, etc.): almost every photochemical oxidation of VOCs involves the production of HCHO. Studies have also shown that agricultural emissions are likely to be another important source of HCHO [1]. Due to the global high level(~2ppm) of atmospheric background methane (CH_4) and its increase trend, 45%~60% of atmospheric background HCHO is ascribed to the following CH_4 involving oxidation processes [2].

$$CH_4 + OH + O_2 \rightarrow CH_3O_2 + H_2O \quad (1)$$

$$CH_3O_2 + NO \rightarrow CH_3O + NO_2 \quad (2)$$

$$CH_3O + O_2 \rightarrow HCHO + HO_2 \quad (3)$$

The sinks of HCHO include its own oxidization or the photolytic processes, and the sink processes also make HCHO an important source of atmospheric CO, these chemical reactions are as the following:

$$HCHO + OH(+O_2) \rightarrow HO_2 + CO + H_2O \quad (4)$$

ISSN 2616-5872 Vol.7, Issue 4: 9-25, DOI: 10.25236/AJEE.2025.070402

$$HCHO + h\nu(+O_2) \rightarrow H_2 + CO \quad (5)$$

$$HCHO + h\nu(+O_2) \rightarrow 2HO_2 + CO \quad (6)$$

HCHO is readily soluble in water as a common formalin solution due to its high Henry's coefficient, and the climate of abundant precipitation or high humidity can be favorable factors for HCHO sinks.

Atmospheric HCHO detection has entered the space age since 1995, when the European Space Agency (ESA) launched the UV-VIS-band hyperspectral probe. Satellites carrying GOME (Global Ozone Monitoring Experiment, 1995-2011)[3], SCIAMACHY (Scanning Imaging Absorption Spectrometer for Atmospheric Cartograp HY, 2002-2012)[4] and OMI (Monitoring Instrument, 2004-present) [5] have given the global distribution of atmospheric HCHO column concentrations [6]. Vegetation and biomass burning in tropical forests and industrial emissions in Africa and South America are the areas of high HCHO column concentrations, as well as the more industrially developed eastern United States of America, eastern China and India. HCHO concentrations in northern Africa are much lower than in the tropical forested regions of Africa due to the extensive arid, desert regions[7]. Since 2006, space observations of HCHO data may also from the GOME-2A/B/C probes on board its satellites (2006-present)[8], Sentinel-5P/ TROPOMI (2018-present) [9], and the OMPS (Ozone Mapping and Profiler Suite) on the NOAA-20 satellite[10]. There are several considerable studies have revealed the characteristics of atmospheric HCHO distribution globally or regionally, especially in the eastern part of China [11] and Indian region [12] where heavily polluted by anthropogenic activities are very obvious.

By using chemical-climate integrated model (RegCM4-CHEM), Saberet found that the high (low) value of HCHO in the Nile Delta appeared in the summer (winter) season and was related to high temperature and high amount of atmospheric OH [13], Moreover, HCHO decreases sharply with the increase of the height of the ground boundary layer. Near-surface measurements in the suburbs of Cairo also found that the highest average of daily HCHO was 32.9±6.6ppbv (summer) the lowest was 18.6±6.9 ppbv (winter), and the average daily concentration was higher than that of many polluted cities in the world[14]. However, there are relatively few studies dealing with the spatial and temporal variations of HCHO over the Egyptian region as well as its long-term trends. In this paper, based on the publicly available multi-satellite remotely sensed data, we analyzed the variation of atmospheric HCHO column over Egypt from 1997-2021 as well as its generally potential sources, exploring the influence of natural and anthropogenic factors on HCHO in the region.

2. Studied Area

Egypt is located in the northeastern Africa, with longitudes and latitudes respectively range of 27.56-35.77°E, 21.6-31.6°N. Egypt spans two continents, Asia and Africa, and its land borders are bounded by Libya in the west, Sudan in the south, the Red Sea, Israel and the Mediterranean Sea respectively in the east, northeast, and the north. The Nile is the main river in Egypt. The land on both sides of the valley has a higher elevation, about 800 m above sea level in the west and 1,000 m in the east. The highest elevation is 2,614 meters at Mount Catherine in the Sinai Peninsula, and the lowest elevation is in a depression in the northwest, 139 meters below mean sea level (see Figure 1). Deserts make up most of the country's vast land. Agricultural land is mainly located on rivers close to the Nile[15]. In Egypt, there are three types of climates: a Mediterranean climate on the northern coast, a tropical desert climate in the interior, and a temperate desert climate along the Red Sea coast [19]. In winter(November to April), the coastal areas are rainy and temperature is 17.4-34.7℃; in summer(May to October), hot and dry and temperature is 9-28.3℃[26]. The average precipitation along the Mediterranean coastline is over 200 mm/year, with most areas receiving only about 2 mm/year away from the coast[19]. Egypt's main crops and plants mainly distribute along the Nile and the northern coast, followed by sporadic distribution of oasis in the central part of the country[33].

About half of Egypt's inhabitants live in urban areas, with the majority spread across densely populated centers in Cairo, Alexandria, and other major cities in the Nile Delta. Agriculture is an important part of the Egyptian economy, providing about 14.5% of GDP and 28% of employment [33]. Egypt is a developing country, ranked 97th on the Human Development Index. Egypt has an uneven distribution of industries, with major industries including textiles, food processing, plastics, iron and steel, automotive, and real estate sectors [32].

Egypt's development was constrained by natural geography environment. With the growth of population and the acceleration of urbanization, the environmental pollution in Egypt is becoming more

ISSN 2616-5872 Vol.7, Issue 4: 9-25, DOI: 10.25236/AJEE.2025.070402

and more serious. Water issues, food security, health security, socio-economic development are all negatively affected by climate change [17]. Egypt is vulnerable to many sustainability challenges and the effects of climate change due to its location in arid and semi-arid regions, the concentration of economic, population, and industrial areas, and the high concentration of natural plants in some cases in the desert.

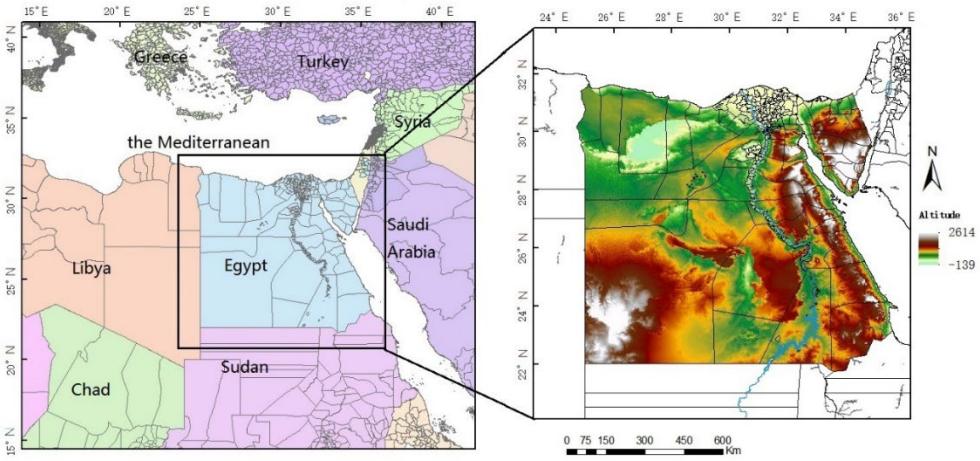

Figure 1: Geographical Distribution of Egypt and Topographical Distribution within Egypt (most of the map).

The reasons for selecting the Egyptian region to analyze the satellite HCHO column concentration products in this paper are: firstly, Egypt is an arid and semi-arid region, and the country is mainly composed of deserts, and climatically it is similar to that of the north-western part of China but hotter and less rainy; secondly, the northern part of Egypt is close to the Mediterranean Sea, a part of the Eastern Mediterranean region, which is one of the famous air pollution areas in summer .There are high values of tropospheric ozone. In addition, Egyptian region is the neighbor of Red Sea-Suez Canal. The development of the world economy is reflected in the pollutant emissions from shipping in the Red Sea. Therefore, the study of the long-term distribution of HCHO in this region can reflect the impact of natural and anthropogenic processes on the atmospheric environment.

3. Data and Methods

3.1 Satellite HCHO Column Data

Atmospheric HCHO column data are from GOME (The Global Ozone Monitoring Experiment), SCIAMACHY (Scanning Imaging Absorption Spectrometer for Atmospheric Cartography) and OMI (Ozone Monitoring Instrument), GOME-2A/2B/C, OMPS, OMPS and TROPOMI, etc. Among these data, the HCHO column concentration on Aura-OMI over China region have been widely analyzed [18]. Table 1 provides a general description of the satellite HCHO products used in this manuscript. It is noted that the HCHO column concentration products used in this paper are from the Ozone Monitoring Instrument OMI (OMI) on board Aura, which is another detector that uses a UV/Vis band spectrometer to observe the solar spectrum backscattered from the Earth's atmosphere to invert the atmospheric column concentrations of trace gases such as O_3, NO_2, HCHO, etc., following the satellite GOME and SCIAMACHY detectors

Table 1: Atmospheric HCHO column concentration data from satellite remote sensing used.

Satellites	periods	resolution	overpass time	Data sources	note
Temis-GOME	1997-2003	0.5°×0.5°	10:30	https://h2co.aeronomie.be/	L3- Monthly average
Temis-SCIAMACHY	2003-2011	0.25°×0.25°	10:30	https://h2co.aeronomie.be/	L3- Monthly average
Temis-OMI	2005-2018	0.25°×0.25°	13:30	https://h2co.aeronomie.be/	L3- Monthly average

ISSN 2616-5872 Vol.7, Issue 4: 9-25, DOI: 10.25236/AJEE.2025.070402

Temis-GOME-2A	2007-2013	0.25°×0.25°	9:30	https://h2co.aeronomie.be/	L3- Monthly average
Temis-GOME-2B	2013-2015	0.25°×0.25°	9:30	https://h2co.aeronomie.be/	L3- Monthly average
GOME-2B*	2013-2022	0.25°×0.25°	9:30	https://acsaf.org/	L3- Monthly average
GOME-2C*	2019-2022	0.25°×0.25°	9:30	https://acsaf.org/	L3- Monthly average
TROPOMI	2019-2021	0.05°×0.05°	13:30	[9]	L3- Monthly average

*Not used for long-term trend analysis

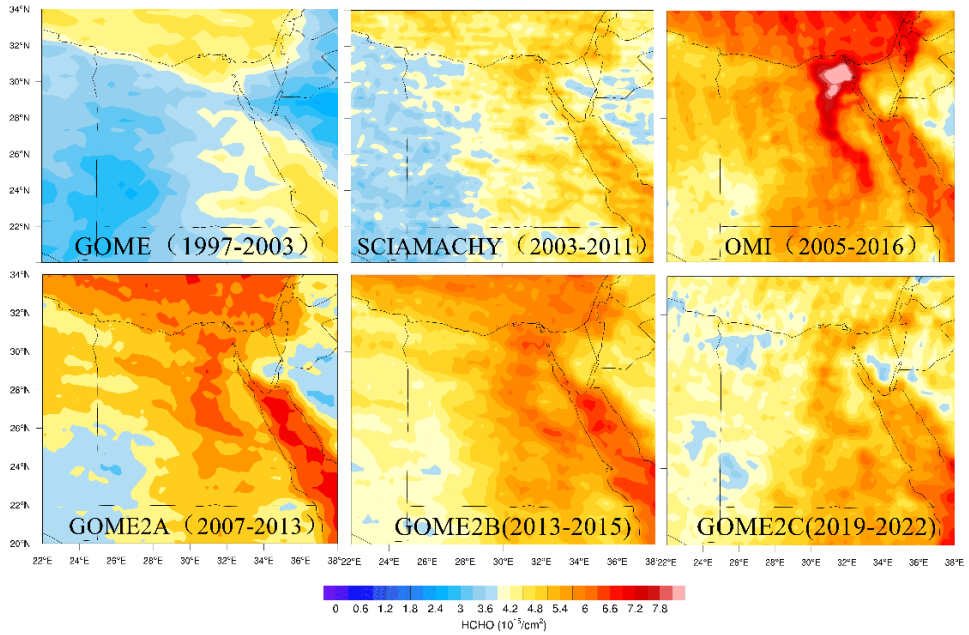

Figure 2: The average concentration of HCHO in Egypt observed by six sensors.

Since satellites detect slant column densities by measuring radiation backscattered from the surface and the atmosphere, air quality factors (AMFs) are then applied to convert them to vertical column densities. These AMFs depend on various factors such as satellite viewing angle, vertical profile of HCHO, clouds and aerosols. However, the AMFs are highly sensitive to the vertical profile of HCHO due to scattering caused by air molecules and the uncertainty of the slant column fit. The provenance of the satellite products listed in the table 1 also means that the inversion algorithms for the data are not the same, and even the HCHO column concentration data products from the same satellite (e.g., OMI or GOME-2B) are different. Differences of HCHO concentration are also due to differences in satellite local overpass time. HCHO in the troposphere is strongly influenced by photochemical reactions, long-term ground-based measurements have shown to be significantly higher at mid-day (e.g., OMI or TROPOMI) than that detected in the local morning.

Figure 2 shows the annual mean distribution of HCHO column concentrations in the Egyptian region detected by the six detectors at different periods of time, as can be seen from the figure, OMI (2005-2018) has the highest mean value followed by GOME-2A (2007-2013). GOME (1997-2003) has the lowest HCHO column concentration due to the different local overpass time. However, all satellites reflect that HCHO in the Egyptian region is highest in the Nile basin and Nile delta region, followed by the southern Mediterranean Sea, the northern African coast, the Red Sea region, and the lowest values in the southwestern desert region. The regional distribution of HCHO in the Egyptian region is in line with expectations: the Nile Delta is the most developed region for agriculture and industry, the Red Sea is also highly influenced shipping, and in the Southwest Desert region there is the least amount of plants and the least amount of HCHO produced by photolysis of biological VOCs.

3.2 Other Data

The meteorological data, ERA5 reanalysis meteorological data from the European Centre for Medium-Range Weather Forecasts (ECMWF) is used, the monthly mean 10m u,v wind field data for

ISSN 2616-5872 Vol.7, Issue 4: 9-25, DOI: 10.25236/AJEE.2025.070402

Egypt and the surrounding area for the years 2012-2021 at a resolution of 0.25° x 0.25°.

Normalized Difference Vegetation Index (NDVI) come from Google Earth Engine. It is a cloud platform provided by Google for online visual computation and analytical processing of a large amount of global-scale geoscience information (especially satellite data), with a spatial resolution of 1000m, a temporal resolution of annual scale, and a selection period of 2017-2020. CH_4 is derived from the Copernicus Atmosphere Monitoring Service(CAMS) global emission inventories, a dataset containing gridded distribution data of global anthropogenic and natural emissions on a month-by-month basis[25].

The Egyptian gross product GDP is used as a representative data for anthropogenic sources, and the data consists of gridded annual datasets from 1990 to 2015, with a spatial resolution of about 1 km. In this study, the data were averaged to monthly and spatially regridded to 0.25° resolution.

We use LandScan Global Population Data (LSGPD) distribution data with a spatial resolution of 1 kilometer, which is the social standard for the release of global LSGPD by the U.S. Department of Energy's Oak Ridge National Laboratory (ORNL), using an innovative methodology that combines the Geographic Information System (GIS) and Remote Sensing (RS). The unit of represent the average or approximation of the population distribution values[20].

3.3 Mathematical Methods

Slope trend analysis is a predictive analytical method that analyzes the amount of change over time in a linear regression to predict its future trend. The formula is as follows:

$$\theta_{\text{slope}} = \frac{n\times\Sigma_{i=1}^{n}(i\times HCHO_i)-\Sigma_{i=1}^{n}i\Sigma_{i=1}^{n}HCHO_i}{n\times\Sigma_{i=1}^{n}(i^2)-(\Sigma_{i=1}^{n}i)^2} \quad (7)$$

θ_{slope} is Slope of HCHO trend per image element, n is the cumulative number of years in the study period, i is year, $HCHO_i$ is the average column concentration of HCHO in year i, θ_{slope}The larger the absolute value, the higher the degree of change. When $\theta>0$, Indicates an increasing trend of HCHO with the time series, instead when $\theta<0$, indicates a decreasing trend in HCHO with the time series.

Mann-Kendall (MK Trend testing method is a non-parametric statistical test that can be used to predict the long-term trends of meteorological factors such as temperature, precipitation and barometric pressure. The MK test does not require the sample data to meet a specific form of distribution, and at the same time will not be disturbed by a small number of outliers. Slope trend analysis provides the specific value of trend change, but it may not be precise enough for nonlinear trend data.MK test provides the reliability and significance of whether there is a trend change in the data or not, but it can't provide the specific value of trend change, so the 2 types of trend analysis are used here[17].

The backward trajectory model adopts the Hysplit model developed by the National Oceanic and Atmospheric Administration (NOAA) of the United States, which is a hybrid Eulerian and Lagrangian atmospheric dispersion model. Its advection and diffusion are handled by the Lagrangian method, and the Eulerian method is used for concentration calculations. The Hysplit model is widely used for analyzing atmospheric pollutant transport paths, and it reflects the spatial trajectory of the air mass. We use 00:00 (UCT) every day as the start time of the hindcast, and use HYSPLIT to simulate the 72-h hindcast trajectories of the daily air movement as well as to cluster the simulated effective hindcast trajectories[21].

4. Result

4.1 Spatial Distribution of HCHO Concentration

Considering the difference in satellite local overpass time, the annual average HCHO concentration from 2005 to 2022 were given out by the OMI and TROPOMI product (Fig3). The range of the average annual concentration of HCHO is 3.71×10^{15}molec/cm^2~9×10^{15}molec/cm^2 as shown in Fig 3. The distribution of HCHO is uneven and has regional characteristics: the peak value is concentrated in the Nile Valley and Nile Delta north of Cairo, followed by the shape of the high value distribution area close to the Nile; HCHO in the northern and eastern coastal areas was at secondary high, and was also higher than that in the southwestern desert. The desert area in the southwest, close to the interior, is always low. HCHO concentrations in Egypt show an increasing trend from 2005-2022, with an increasing area of peak values, expanding from the Nile Delta to the coastal areas.

ISSN 2616-5872 Vol.7, Issue 4: 9-25, DOI: 10.25236/AJEE.2025.070402

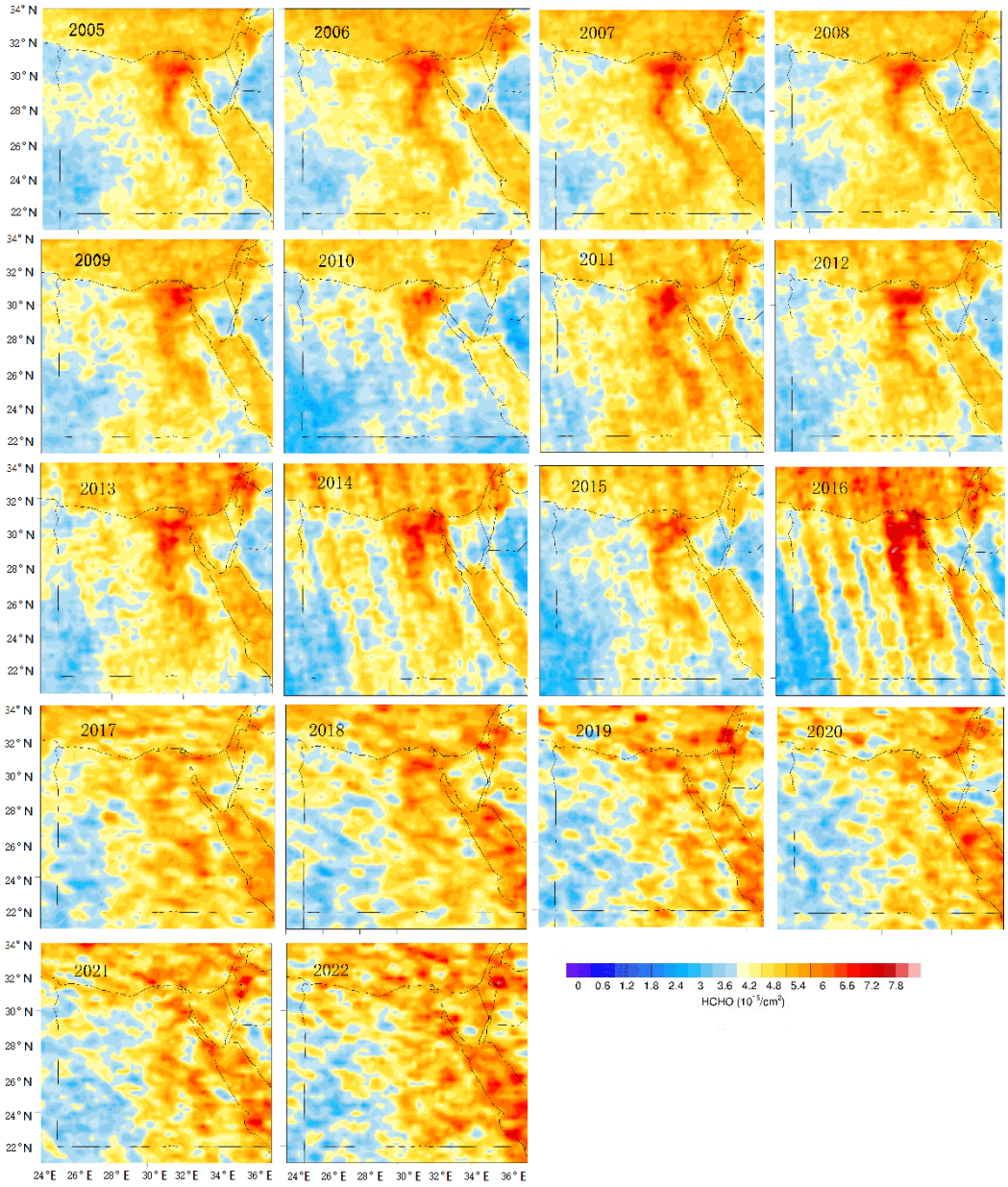

Figure 3: Annual mean distribution of HCHO in Egypt from 2005 to 2022

4.2 Comparisons of Yearly Average of multi-satellite satellite HCHO

Figure 4 shows the variation of the annual average of HCHO column concentrations in the Egyptian region as revealed by the satellites listed in Table 1. The study shows[22] that the OMI detector is not recommended to be used after 2018 because of the aging of the instrument and the anomalies in the line data; similarly the GOME2A detector also shows significant aging in 2019 and makes the HCHO appear anomalously high values, while GOME-2C (2019-2022) shows an unknown cause minimum. However, all the combined data together indicate an increasing process in the column concentration of HCHO over the Egyptian region. Therefore, this paper analyses the variation of HCHO concentration in the Egyptian region over the last 25 years using the combined annual mean HCHO column concentration data values of GOME, SCIAMACHY, GOME-2A and GOME-2B in Table 1.

ISSN 2616-5872 Vol.7, Issue 4: 9-25, DOI: 10.25236/AJEE.2025.070402

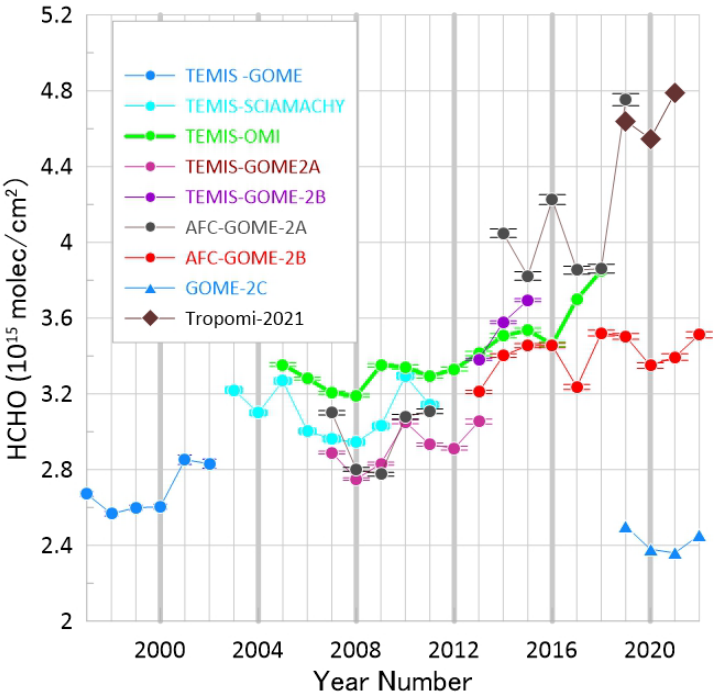

Figure 4: Variation of annual mean column concentrations of HCHO in the Egyptian region based on the satellite sensors listed in Table 1.

4.3 Geographical Distribution of Averaged HCHO in Summer and Winter

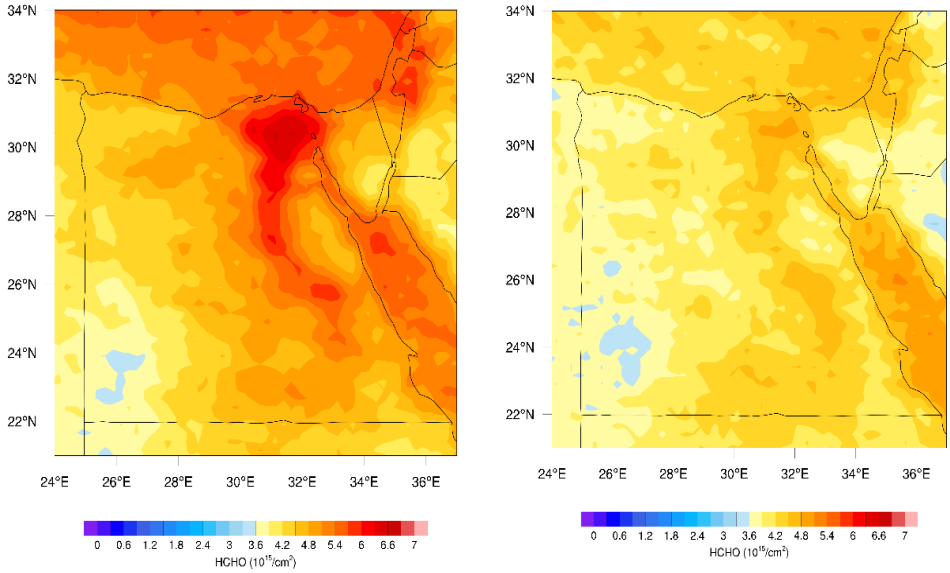

Figure 5: The geographical distribution of averaged composite HCHO column concentration values in summer (May-October) (left) and winter (November-April) (right) in Egypt.

The seasonal variation of HCHO in Egypt was obvious as shown in Figure 5. The peak value was concentrated in the Nile Valley and Nile Delta north of Cairo. The average range in summer is 3.2--6.8×10^{15}molec/cm^2, and the average range in winter is 2.6-4.8×10^{15}molec/cm^2. The geographical gradient difference of HCHO is obvious in summer but in winter. In the Mediterranean Sea and the Red Sea, of HCHO concentration is higher in summer than in winter.

Schaber[13] pointed out that the higher value of HCHO occurs in summer in the Nile Delta area while the lowest in winter. The average concentration of HCHO was significantly lower out of urban sites. For an example, surface observation in suburban Cairo reached 32.9±6.6×10^{15}molec/cm^2 in summer [14],

ISSN 2616-5872 Vol.7, Issue 4: 9-25, DOI: 10.25236/AJEE.2025.070402

indicating that the increase in traffic density around observation site not only increases the emission of HCHO in exhaust gas (primary source),= but also of VOCs(secondary source), which plays an important role in the photochemical production of HCHO, is increased.

Liu et al [24]extracted and analyzed tropospheric HCHO column concentration data in China from 2015 to 2017 based on satellite data, and the results showed that the seasonal mean value of HCHO column concentration in China was 11.26×10^{15}molec/cm^2 in summer > 10.20×10^{15}molec/cm^2 in spring > Autumn (9.70×10^{15}molec/cm^2)> Winter (9.68×10^{15}molec/cm^2). It also showed that the photochemical processes of atmospheric pollutants are strengthened in different regions with high solar radiation intensity in summer, and the ground-based HCHO ranged from 1.27 ± 0.15~$21.98\pm6.80\times10^{15}$molec/cm^2, while the observation data at the upper were relatively stable, indicating variation of HCHO column data mainly reflect the changes in planetary boundary -layer that is closed with anthropogenic activities.

4.4 Trend Analysis

The slope trend analysis suggest that the high slope values are found in the Nile delta and the northernmost part of the Red Sea, and the slope index shows an increasing trend there (Figure 6-left).The Mann Kendall (MK) test was also performed to analyze the spatial distribution of the trend of HCHO column concentration, and the results reveals that the MK values show higher positive values in the Nile Delta and the northern Red Sea coast is also obvious(Figure 6-right), with the highest positive value of 1.5~2.9, which indicates a obvious increasing trend in the region. The MK values gradually increase from the southwest to the northeast .There is a high degree of similarity between MK test and slope trend analysis.

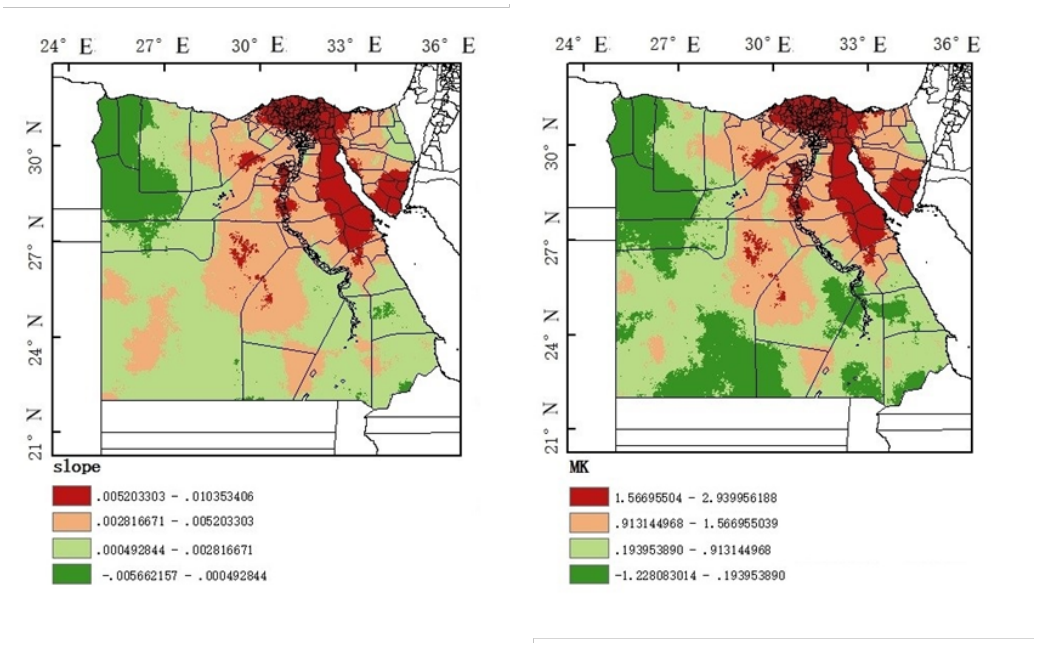

Figure 6: Distribution trend of slope coefficient (right) and MK coefficient (left) of multi-satellite HCHO column data over Egypt and its surrounding areas.

The global products of GOME (1996.6-2003.06), SCIMARCHY (2003.01-2012.03), GOME-2A (2007.01-2013.12) and GOME-2B (2013.01-2022.12) mentioned in Table 1 are composed to determine the long-term variation of atmospheric HCHO column concentration in the Egyptian region. These satellite products were selected due to their close overpass time over the Egypt and the same retrieval algorithm of the products [8], which reduces the differences between the different satellite products and improves the consistency, thus facilitating the assessment of the characteristics of the long-term trend of atmospheric HCHO column concentration. The data were processed by averaging the global HCHO column concentrations of the satellites with the same year and month to establish a series of monthly average column concentrations from 1997.01 to 2022.12, based on which the annual average of HCHO column concentrations were extracted from the whole Egyptian territory and from representative locations (see Table 2) in different climatic zones of Egypt (see Figure 7) according to the distribution of latitude and longitude grid points.

ISSN 2616-5872 Vol.7, Issue 4: 9-25, DOI: 10.25236/AJEE.2025.070402

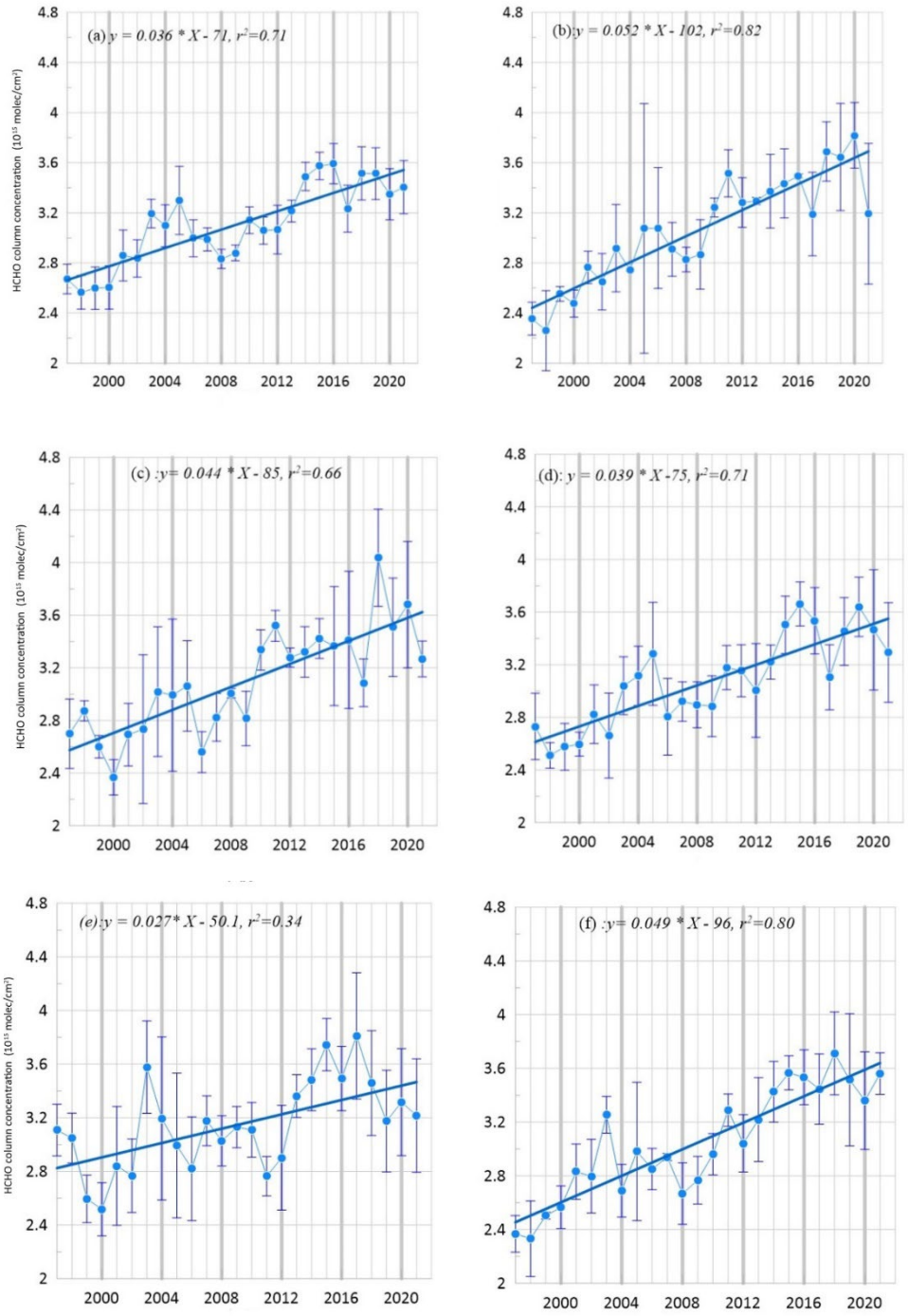

Figure 7: Trends in annual mean column concentrations of HCHO in Egyptian regions from 1997-2022.

(a) Egypt as a whole; (b) the Nile Delta region (Cario and Damietta), (c) the cities along the Mediterranean Sea in northwestern Egypt (Marsa Matruh, Alexandria,), (d) oasis areas in western or southern Egypt (Siwa, Bahariya, Bahrien, Farafra, Faiyum, Kharga Dakhla, Aswan, Luxor), (e) the uninhabited areas of south-west Egypt close to the Hazara Desert, and (f) the three port cities of the Red Sea and the Suez Canal (the port cities of El Tor, Suez and Said).

Figure 7 gives the trend of annual mean HCHO column concentrations in Egypt (1997-2021), including the whole Egyptian territory and five geographically or climatically differentiated regions. It can be seen that the average annual growth rate of HCHO over the whole Egyptian territory is 0.036×10^{15}molec/cm^2/year over 25 years (Fig. a); the Nile Delta region, represented by the cities of Cario

ISSN 2616-5872 Vol.7, Issue 4: 9-25, DOI: 10.25236/AJEE.2025.070402

and Damietta, has the largest growth rate of 0.052×10^{15}molec/cm^2/year (Fig. b), followed by the Nile delta region represented by Eltor, Suez, and Said, which represents the Red Sea-Suez region (Fig. c), and the Nile Delta region represented by Eltor and Suez, which represents the Red Sea-Suez region (Fig. d). Suez and Said representing the Red Sea-Suez Canal region with a growth rate of 0.049 $\times10^{15}$molec/cm^2/year (Fig. f). The southern Mediterranean coast of NW Egypt represented by Marsa Matruh and Alexandria has a growth rate of 0.044 $\times10^{15}$molec/cm^2/year (Fig. c). The average growth rate of the eight oasis regions (consisting of Siwa, Faiyun, Bahariya, Farafran, Kharga, Dakhla, and the Nile Valley cities of Aswan and Luxor in the south of Egypt) was 0.039×10^{15}molec/cm^2/year (Fig. d), which is the closest to the average for the whole of Egypt. The lowest growth rate of 0.027 $\times10^{15}$molec/cm^2/year was found in the unoccupied area of south-west Egypt near the Hazara Desert (Fig. e). In addition, Figure 7 shows that there are two peaks in the annual mean values of HCHO in the whole Egyptian territory and representative sites of oases and deserts, in addition to a clear increasing trend: 2002-2004 and 2014-2016, with a difference of about 11 years, which is close to the solar activity cycle. This phenomenon is also present but not significant in the Red Sea-Canal region, and not in the Mediterranean coast of north-west Egypt and the Nile Delta. These phenomena may reflect the long-term variations in HCHO concentrations regionally controlled by tropical desert arid and Mediterranean climates, respectively.

Figure 7 also reveals that the differences in the average annual growth rates of HCHO in different regions of Egypt are closely related to the natural environment and economic development of each region:the Nile Delta region concentrates Egypt's industrial, agricultural and densely populated environments, and the 1st and 2nd source values of HCHO are higher, so HCHO presents higher concentration values [14], and this high value characteristic of HCHO and high annual growth rates has been reflected in the long-term measurements of satellite as well. The next highest annual growth rates in the Red Sea and Suez Canal Basin are also closely related to primary sources from fossil fuel combustion for shipping. In contrast, in desert or oasis areas, the overall annual growth rate of HCHO is relatively low, despite localized emissions from HCHO BVOC sources. In terms of HCHO growth rates, anthropogenic primary source emissions have a significantly higher impact in the Egyptian region than BVOC source contributions.

Since atmospheric temperature, humidity, precipitation, and methane oxidation (chemical reactions (1)-(3)) all have an effect on HCHO concentration variations, in order to further understand the relationship between long-term HCHO variations in different geographic environments of the Egyptian region and these factors, Table 2 gives a more refined comparison of the mean annual growth rate of HCHO concentration and the correlation between the mean annual column concentration values and temperature, relative humidity, precipitation, and methane.

Table 2: Satellite HCHO annual growth rate (1997-2021) correlations (r2)with meteorology.

region	location	growth rate (10^{15} moles cm^{-2}.y^{-1})	vs.Temp.	vs.RH*	vs. Precip*
All	all Egypt	0.036	0.484	0.245	0.282
Nile Delta cities	Cairo(31.28°E ,30.08°N)	0.049	-	-	-
	Damietta(31.814°E, 31.418°N)	0.055	-	-	-
Mediterranean Port cities	Marsa Matruh(27.237°E, 31.354°N)	0.044	0.18	0.243	0.127
	Alexandria(29.918°E, 31.2°N)	0.044	-	-	0.117
Oasis and middle Nile Valley area	Siwa(25.532°E, 29.180°N)	0.04	-	0.339	-
	Faiyun(30.582°E, 29.353°N)	0.055	0.25	0.162	-
	Bahariya(28.909°E, 28.385°N)	0.02	0.419	0.137	0.174
	Farafran(26.764°E, 26.953°N)	0.051	0.243	0.335	-
	Dakhla(28.97°E ,25.49°N)	0.04	0.357	0.117	0.149

ISSN 2616-5872 Vol.7, Issue 4: 9-25, DOI: 10.25236/AJEE.2025.070402

	Kharga(30.54°E ,25.449°N)	0.038	0.328	0.281	-
	Aswan(32.52°E, 23.58°N)	0.032	0.153	-	0.132
	Luxor(32.64°E, 25.687°N)	0.034	0.349	0.106	0.198
Desert	Desert#2 (25.4°E, 22.4°N)	0.027	0.171	0.134	-
Red Sea - Suez Canal Zone	Eltor(33.623°E ,28.241°N)	0.038	-	-	-
	Suez port(32.54°E, 29.98°N)	0.054	-	-	-
	Said port (32.27°E, 31.25°N)	0.056	-	-	-

*Squared values of negative correlation coefficient; "-" represents no significance in the correlation.

As can be seen from Table 2, the highest average annual growth rates are found in: Said, Damietta and Faiyun Oasis, followed by the port of Suez. The high value of shipping ports should be closely related to the development of shipping driven by the global economy. The oases of Faiyun and Farafran also show a high value of 0.05 $\times 10^{15}$molec/cm^2/year whether the economic development or not is yet to be further analyzed. The rate of Bahariya oasis has the lowest mean annual value in the linear fit because of the high value of 3.6×10^{15}molec/cm^2/year in 2005 and the correlation coefficients are also low. It can also be seen from Table 2 that the annual growth rates of HCHO are lower south of 25°N, although this region is closer to the zone of high HCHO column concentrations in the tropical equatorial low latitudes of Africa [9]. The correlation between annual mean HCHO and annual mean air temperature is not correlated in the Nile Delta region, the canal harbour, and also in Alexandria and Siwa Oasis, reflecting the fact that the increasing trend of HCHO concentration is more influenced by primary sources, and it needs to be further explored whether the absence of correlation in Siwa Oasis is related to the altitude of this oasis area below sea level or other factors, but the significant correlation between HCHO and temperature in the other areas (oases and deserts) should reflect the fact that temperature is one of the mechanisms influencing the changes in HCHO concentration. Mechanisms include increased emissions of BVOCs and thus increased photochemical production of HCHO as a result of rising temperatures, and increased participation of HCHO in atmospheric photochemical processes as a result of rising temperatures under adequate sunlight.

As with the correlation between HCHO and temperature, none of the annual means of HCHO and relative humidity in urban areas with significant primary source emissions showed a correlation, nor was there a significant correlation in the Aswan region. Because of the overall decreasing trend of relative humidity in ERA5 over the 25-year period in Egypt or in desert and oasis areas (figure omitted), the overall decreasing trend of relative humidity in urban and harbour areas (except for Marsa Matruh) is not significant, probably due to significant anthropogenic activities; and in the Aswan region, due to the moderating effect of evaporation from the water surface of the huge reservoirs on the background humidity in the atmosphere, the relative humidity does not show a significant decreasing trend either. The Aswan region did not show a significant decreasing trend in relative humidity because of the moderating effect of the huge reservoir water surface evaporation on the atmospheric background humidity, thus making the correlation between HCHO and humidity not obvious. The correlation mechanism between annual average HCHO and total annual precipitation is similar, but the correlation with HCHO in deserts and most of the oasis areas is also not obvious because the total annual precipitation is too low.

ISSN 2616-5872 Vol.7, Issue 4: 9-25, DOI: 10.25236/AJEE.2025.070402

5. Influencing Factors of HCHO

5. 1 Vegetation Coverage From the NDVI

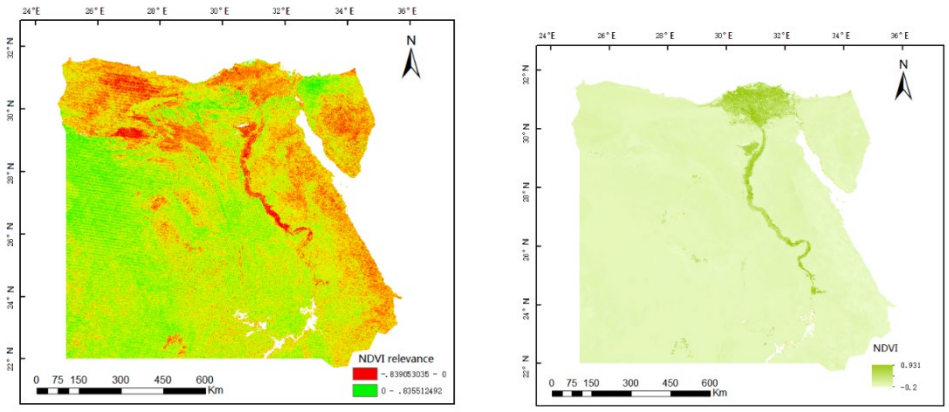

Figure 8: NDVI coefficient distribution in Egypt and its surrounding areas (right) and correlation coefficient between HCHO column concentration and NDVI (left)

Vegetation has the ability to alter the carbon cycle and stabilize the climate system, acting as a transmitter of material cycles and energy flows in the ecosystem. While absorbing, degrading and purifying atmospheric pollutants, plants can generate isoprene and other BVOCs through the action of enzymes in the chloroplasts of plants, and release them into the atmosphere through the stomata, where they react with O_3 and OH to produce a large amount of oxidizing substances, and HCHO is the main intermediate product of BVOCs oxidation, so isoprene can promote HCHO. HCHO is the main intermediate product of BVOC oxidation, so isoprene can promote the direct release of HCHO[27]. At the same time, studies have shown that meteorological conditions such as temperature and precipitation can also have an important effect on HCHO, so this section specifically analyzes the spatial correlation between NDVI and HCHO column concentrations.

The NDVI is a standardized index used to express the amount of vegetation, reflecting plant growth patterns and the extent of vegetation cover. As shown in the figure 8 right, vegetation is mainly concentrated in the Nile region of Egypt[28]. The areas of highest predicted species richness are located in northeastern Egypt, especially from the Sinai Peninsula in the north to the mountains in the south, along all borders between Egypt and Israel, along the Mediterranean coast from Rafah to Port Said, and along the Red Sea. Species richness decreases from northeast to southwest, with species richness approaching zero in the vast majority of Egypt's interior. The positive correlation area in Egypt was set to be green, accounting for 63.45% of the total, mainly in the northern coastal area, the Nile coast and Nile estuary delta, the southern Sinai Peninsula, and the eastern coastal area. In figure 8 (left)HCHO and NDVI correlation coefficients ranged from -0.84 to 0.835 with strong correlation. It shows that vegetation cover will increase local HCHO.

5.2 Wind vector on the 850hPa Isobaric Surface

Transport in the atmospheric circulation has a significant effect on the changes in the distribution of pollutant concentrations. Figure 9 shows the distribution of mean wind vector values over the 850 hPa isobar in summer and winter. During the summer season, the predominantly prevailing winds over Egypt are northerly and northwesterly in the Mediterranean region, and the winds move westward from the Mediterranean region to Iraq, and then advance to the southwest in the Saudi Arabia region, and finally undergo a change in the wind direction in the Red Sea waters. Meanwhile, the high altitude of western Egypt and the Red Sea block the interference of winds from the Saudi Arabian region. During the winter months, the main pressure systems affecting the weather in Egypt are the subtropical high pressure, the Red Sea Trough (a northward extension of the Sudanese monsoon low pressure) and mid-latitude cyclones. Winds are generally westerly over the Mediterranean, northwesterly over northern Egypt, and northeasterly over southern Egypt.

ISSN 2616-5872 Vol.7, Issue 4: 9-25, DOI: 10.25236/AJEE.2025.070402

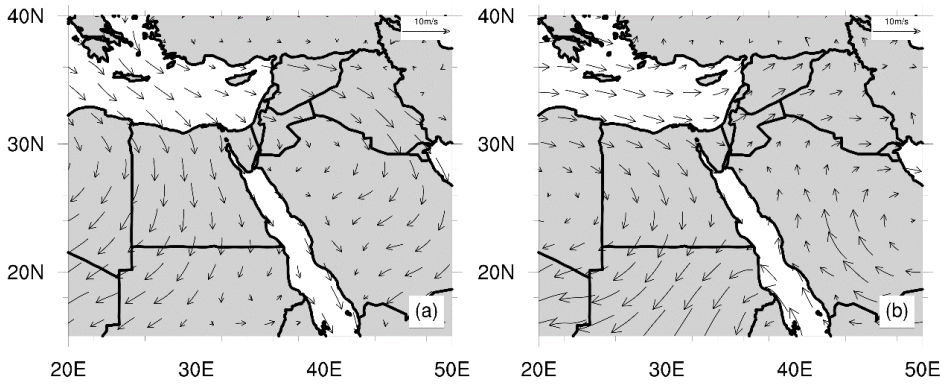

Figure 9: Average wind field distribution at the 850hPa isobaric surface over Egypt and surrounding areas in summer (May-October, Left) and winter (November-April, Right).

5.3 Pollutant Transport and Potential Source Areas

According to the economic development and geographic locations of the urbanization, the high-value area is located in the Nile Delta in the northern part of Egypt, which is at a high level of the year-round HCHO column concentration value, so a typical city: Cairo (30.03°N, 31.23°E), is selected as a focal point in the region. May-October for summer and November-April for winter. In May-October (November-April), the average temperature is 17.4-34.7°C(9-28.3°C), the average precipitation is about zero(3.8m^2), and the average sunlight hours are all above 9 (7) hours, where the highest solar UV irradiance months are June and July (December.) (weather atlas, 2023).

Seven -two hours of backward trajectory of day by day is simulated. The starting height of each trajectory is chosen at 500m above the ground for reflecting the average flow field characteristics of the boundary layer. The directions of transport of backward trajectory are determined by the Angle Distance algorithm, for the clustering analysis of the trajectory (fig 10 a and b) .

During the summer months, the trajectories are mainly from the north-west. Type 1 trajectory sources are mainly from the northwestern direction, with the longest transmission distance, and are air flows are from the Mediterranean Sea, with the farthest end extending to the ocean north of Tunisia, with a share of 9.39%; Type 2 trajectory sources are mainly from slightly shorter distances, coming from the due-north direction, and with the farthest end passing through Turkey, with a share of 35.36%; Type 3 trajectories crossing the Antikythera Strait, with the end approaching the southwestern part of Italy. 28.18%; category 4 trajectories are mainly from the due north direction and the flow is mainly from the western Turkish border, 27.07%.

During the winter season, category 1 sources are mainly from the Sinai Peninsula and Israel, with a share of 28%, over very short distances; category 2 sources are mainly from the Mediterranean Sea, extending as far north as the Sicilian region of Italy, with a share of 30.39%; category 3 sources are mainly from due north as far as Bulgaria; and category 4 sources are mainly from the coastlines of Egypt and Libya, with a share of 16.57%.

Part of the Sinai Peninsula of Egypt is mountain Mount area, and the relatively high elevation of the coast on the western side of the Red Sea creates a natural barrier, so that atmospheric pollutants in the Cairo area are susceptible to the Mediterranean climate to the north. During the summer months, a persistent pressure gradient extends from the Atlantic Ocean to the Asian low, producing the Etesians winds. It is affected by biomass burning activities[29]. The eastern Mediterranean is bounded by a more or less flat desert in the south, so that in summer it is exposed to the Asian monsoon system[30]. The Etesian wind is the prevailing wind blowing from the north or northwest of the Aegean Sea. They are produced by a combination of high pressure over the Balkans and low pressure over Turkey. The direction of the wind is from the Aegean Sea to the southeast[31]. Overall, in the Mediterranean, the months with the highest wind speeds are December and February. The highest wind speeds (up to 8.8 m/s) occurred in December off shore Lion Bay and in February in the Aegean Sea (up to 8.2 m/s). The next months with the highest winds are January and March. In addition, from June to September, wind conditions were generally calm in most parts of the Mediterranean, except the Aegean Sea. Mainly in July and

ISSN 2616-5872 Vol.7, Issue 4: 9-25, DOI: 10.25236/AJEE.2025.070402

August, the Etesia winds prevail in the area[23]. In the summer of May to October, the range of potential sources is more to the west and north than in the winter, and the red zone can reach the Aegean Sea and north of Turkey. In winter, the wind from the eastern Mediterranean is relatively strong, generally speaking, the concentration of atmospheric pollutants is negatively correlated with the wind speed, and the range of potential sources of atmospheric pollutants is mainly concentrated in northern Egypt.

Sabolis et al., found that volatile organic compounds such as isoprene produced by plankton in seawater were the main contributors to the concentration of HCHO column, and HCHO were also closely related to organic aerosol, Marine surface chemical reaction and atmospheric transport[16]. Studies have shown that during the ocean-atmosphere exchange process, HCHO in seawater can be released into the atmosphere to form gaseous HCHO, which has an impact on the variation of HCHO column concentration over the continent. The meteorological and chemical conditions of the Mediterranean summer are conducive to the accumulation of pollutants from primary emissions and the formation of secondary gases and aerosols. Due to the high intensity of solar radiation, the photochemical production of the secondary pollutants are enhanced [34]. It shows that the Marine factors have a certain uplifting effect on HCHO in the northeast of Egypt.

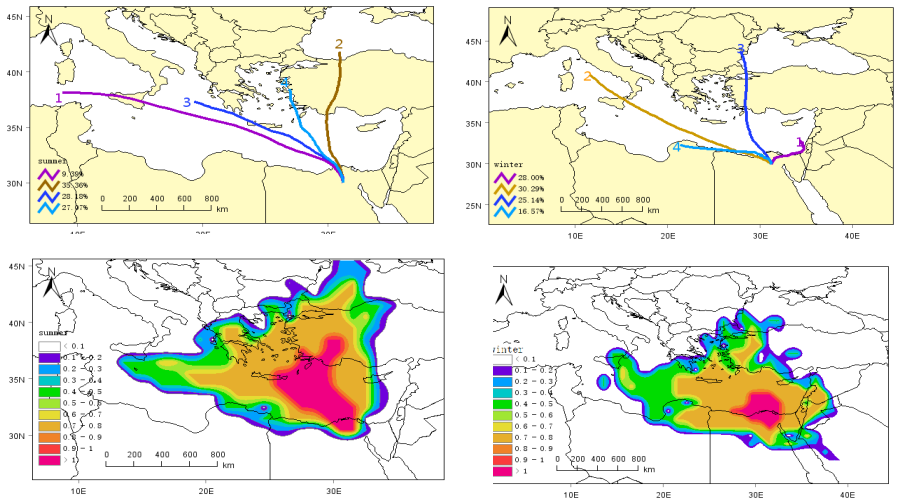

Figure 10: Backward trajectories of 72-hours air mass over the Cairo in summer (up left) and winter(up right),showing respective potential sources of HCHO.

6. Conclusions

Multiple satellites observation atmospheric HCHO from over Egypt from 1997 to 2022 are presented and analyzed. The average annual average HCHO concentration in Egypt ranges from 3.71×10^{15}molec/cm^2 to 9×10^{15}molec/cm^2. The peak value of the mean value is concentrated north of Cairo in the Nile Valley and the Nile Delta, followed by the shape of the high value distribution area close to the Nile; The concentration in the northern and eastern coastal areas is at secondary position, and the desert area in the southwest near the inland is the lowest. The concentration of HCHO in Egypt is higher in summer than in winter, and the growth rate is stable.

Temporal-spatial distribution of HCHO is mainly influenced by natural factors and human factors. The northern coastal area of Egypt has a superior geographical location, sufficient labor force and rapid economic development, and human production activities, all of these factors have a prominent impact on atmospheric HCHO. At the same time, Egypt borders the Mediterranean Sea in the north and the Red Sea in the east, and natural factors also have a certain impact on atmospheric HCHO. The influence of Marine factors on HCHO concentration is more complex. In the Sinai Peninsula region, the Mediterranean coast, the Red Sea coast area rich in vegetation, easy to produce HCHO.

The wind direction on the Mediterranean is mainly western northwestern. After entering Egypt continent, the wind direction turns southward, carrying HCHO pollutants from the Nile Delta region and Sinai Peninsula to the south, while in the southwest of Egypt, which is mainly a desert area, the HCHO concentration is lest, and the final gradient difference is formed.

The concentration of HCHO in the Mediterranean Sea was $6.08\pm0.11\times10^{15}$molec/cm^2, and the

ISSN 2616-5872 Vol.7, Issue 4: 9-25, DOI: 10.25236/AJEE.2025.070402

analysis showed that HCHO on all Marine routes is increasing, and the trend was statistically significant. The ocean characteristics and climatic conditions affects the diffusion and sedimentation of atmospheric pollutants in nearby areas, and the higher HCHO concentrations in coastal areas reflect emissions associated with shipping and seaports, high solar radiation intensity in summer, and enhanced photochemical processes that produce secondary pollutants including HCHO.

Acknowledgement

Statements and Declarations Conflict of interest. The authors declare no competing interests.

Funding This work was funded by Lanzhou Science and Technology Plan Project (2017-RC-69)and the National Natural Science Foundation of China (2016YFC0500907)at the Key Laboratory of Resource Environment and Sustainable Development of Oasis, Gansu province, and the Gansu Province Environmental Science and Engineering Demonstration Laboratory.

Data Availability

The data used in this study were derived from available public domain

Author Contributions

Guanghui Zheng: methodology, writing-original draft review and editing, data curation, resources, visualization, formal analysis.

Tianzhen Ju: project administration, conceptualization, writing-review and editing, methodology, supervision.

Yumeng Qiu writing-review and editing, data curation.

Zhichao Lv: writing-review and editing,investigation, formal analysis

Jiachen Li: writing-review and editing, investigation, formal analysis.resources, data curation.

Data availability

The air pollutant data used during this study are from the NASA, and other datasets analyzed are available from the corresponding author on reasonable request.

Ethical Responsibilities of Authors

“All authors have read, understood, and have complied as applicable with the statement on "Ethical responsibilities of Authors" as found in the Instructions for Authors".

Consent to Participate

This paper does not require consent to participate.

References

[1] Kaiser, J., Wolfe, G. M., Bohn, B., et al.,. Evidence for an unidentified non-photochemical ground-level source of HCHO in the Po Valley with potential implications for ozone production[J]. Atmos. Chem. Phys., 2015, 1289–1298,

[2] Lieschke, K.J., Fisher, J.A., Paton-Walsh, C., et al.. Decreasing trend in HCHO detected from 20-year record at Wollongong, Southeast Australia[J]. Geophys. Res. Lett,2019, 46, 8464–8473

[3] Abbot, D. S., Palmer, P. I., Martin, R. V., Cet al., A.: Seasonal and interannual variability of North American isoprene emissions as determined by HCHO columns measurements from space[J]. Geophys. Res. Lett. 2003., 30, 1886,

[4] Stavrakou, T., Mu¨ller, J.-F., De Smedt, I., et al., Global emissions of non-methane hydrocarbons

ISSN 2616-5872 Vol.7, Issue 4: 9-25, DOI: 10.25236/AJEE.2025.070402

deduced from SCIAMACHY HCHO columns through 2003–2006[J]. Atmos. Chem.Phys. 2009., 9, 3663–3679,
[5] Müller., Potosnak, M. J., Rinne, J., Munger, B., et al., Global isoprene emissions estimated using MEGAN, ECMWF analyses and a detailed canopy environment mode[J]. Atmos. Chem. Phys. 2008, 8, 1329–1341.
[6] De Smedt, I., Mu¨ller, J.-F., Stavrakou,T., et al.. Twelve years of global observations of HCHO in the troposphere using GOME and SCIAMACHY sensors[J]. Atmos. Chem. Phys., ,2008 8, 4947–4963,
[7] Yang Liu, et al.,.Spatio-temporal distribution and source partitioning of HCHO over Ethiopia and Kenya[J]. Atmospheric Environment,2020 237.
[8] De Smedt, I., Van Roozendael, M., Stavrakou, T., et al., Improved retrieval of global tropospheric HCHO columns from GOME-2/MetOp-A addressing noise reduction and instrumental degradation issues[J]. Atmospheric Measurement Techniques, 2012. 5(11), 2933–2949.
[9] De Smedt, I., Pinardi, G., Vigouroux, C., et al.,. Comparative assessment of TROPOMI and OMI HCHO observations and validation against MAX-DOAS network column measurements[J]. Atmospheric Chemistry and Physics, 2021, 21(16), 12561–12593.
[10] Nowlan, C. R., Gonzalo González Abad, Hyeong-Ahn Kwon, et al.,.Global HCHO Products From the Ozone Mapping and Profiler Suite (OMPS) Nadir Mappers on Suomi NPP and NOAA-20[J] .Earth and Space Sience2023,10,5,Pp. e2022EA002643.
[11] XIE Shun-tao, JU Tian-zhen, GE Jian-tuan, et al. Spatial and temporal distribution and related factors analysis of HCHO in China, based on satellite remote sensing China Environment Science[J]. 2018.38(5): 1677–1684.
[12] Kuttippurath J., et al. Investigation of long–term trends and major sources of atmospheric HCHO over India[J]. Environmental Challenges. 2022 ,100477
[13] M.L. Eladawy, H. A. Basset, Mostafa Morsy & M. H. Korany. Study of trend and fluctuations of global solar radiation over Egypt[J] . NRIAG Journal of Astronomy and Geophysics, 2021 10:1, pages 372-386.
[14] Salwa K. Hassan, et al. Effect of Seasonal Variation on the Levels and Behaviours of HCHO in the Atmosphere of a Suburban Area in Cairo, Egypt[J]. Asian Journal of Atmospheric Environment,2018.: 12.4.
[15] Ahmed Nagy Yassen, et al.. Impact of climate change on reference evapotranspiration in Egypt[J]. Catena,2020,194.
[16] Elina Marmer, and Bäerbel Langmann. "Impact of ship emissions on the Mediterranean summertime pollution and climate: A regional model study." [J]. Atmospheric Environment 39.26(2005).
[17] U.S. Department of Agriculture, Foreign Agriculture Service[J]. Egypt, 2025.
[18] UNDP (United Nations Development Programme). Human Development Report 2025: A matter of choice: People and possibilities in the age of AI. New York, 2025.
[19] Ministry of Foreign Affairs of the Netherlands (MFA), Climate change profile: Egypt[J]. Ministry of Foreign Affairs of the Netherlands. 2018.
[20] Jing Zhao.. Egypt's Participation in Global Climate Governance: Perceptions, Practices and Motivations[J]. Arab World Studies, 2022,06:110-132+158.
[21] Ministry of Foreign Affairs of the Netherlands (MFA), Climate change profile: Egypt. Ministry of Foreign Affairs of the Netherlands. 2018.
[22] Liu Dongyang, et al.. Sources and budget analysis of ambient HCHO in the east-central area of the yangtze River Delta region n, China." [J]. Atmospheric Environment, 2023,305.
[23] Sabolis A., et al. "Interpreting elevated space-borne HCHO columns over the Mediterranean Sea using the OMI sensor." [J] Atmospheric Chemistry and Physics,2011, 11.254.
[24] Kummu, Matti; Taka, Maija; Guillaume, Joseph H. A., Data from: Gridded global datasets for Gross Domestic Product and Human Development Index over 1990-2015[J]. Dryad, Dataset, 2020.
[25] Zhao Shuangqing, Wen Wen, Yu Ningyu et al., Analysis of annual precipitation based on Wavelet and MK test. Journal of Hebei University of Technology (Natural Science Edition). 2020, 37(01): 84-90.
[26] Draxler, R. R. and Rolph, G. D. HYSPLIT (Hybrid Single-particle Lagrangian Integrated Trajectory). NOAA Air Resources Laboratory, Silver Spring, MD. 2015.
[27] Yuhan Shi, Shanshan Wang, Sanbao Zhang, et al., HCHO and NO2 profile characteristics under different synoptic patterns in Shanghai, China[J]. Journal of Environmental Sciences, Volume 156,2025,Pages 821-834.
[28] Gopikrishnan G.S., and Kuttippurath Jayanarayanan. A decade of satellite observations reveal significant increase in atmospheric HCHO from shipping in Indian Ocean." [J] Atmospheric Environment 2021,246.
[29] Xiaoyan Tang. Atmospheric Environmental Chemistry,[M]Peking University Press, 2006.
[30] M. Menendez, et al. High-resolution sea wind hindcasts over the Mediterranean area. Climate

ISSN 2616-5872 Vol.7, Issue 4: 9-25, DOI: 10.25236/AJEE.2025.070402

Dynamics,2014, 42,7-8.
[31] Mu¨ller, J.-F., Stavrakou, T., Wallens, S., De Smedt, I., Van Roozendael, Takvor Soukissian, et al. Offshore wind climate analysis and variability in the Mediterranean Sea[J]. International Journal of Climatology,2018, 38.1.
[32] Egypt Human Development Report[R]. United Nations Development Programme,2021.
[33] Human Development Insights[R]. United Nations Development Programme, 2023.
[34] Mostafa Soha M., et al. Potential Climate Change Impacts on Water Resources in Egypt[J]. Water 2021,13.12.